Structural characterization and phase transformations in metal oxide films synthesized by Successive Ionic Layer Deposition (SILD) method

Ghenadii Korotcenkov[1,2,*], Sang Do Han[3], Beongki Cho[2,*], Valeri Tolstoy[4,*]

[1]*Department of Microelectrinics, Technical University of Moldova, Bld. Stefan cel Mare, 168, Chisinau, 2004, Republic of Moldova*

[2]*Department of Material Science and Engineering, Gwangju Institute of Science and Technology, 1 Oryong-dong, Buk-gu, Gwangju, 500-712, Republic of Korea*

[3]*Future Fundamental Technology Research Department, Korea Institute of Energy Research, 71-2 Jang-dong, Yuseong-gu, Daejeon, Republic of Korea*

[4]*Department of Solid State Chemistry, Institute of Chemistry, St. Petersburg State University, University St. 26, St. Peterhof, St-Petersburg, 198504, Russia*

Received 13 August 2008; received in revised form 2 February 2009; accepted 23 February 2009

Abstract

In this paper the peculiarities of phase composition and morphology of metal oxides synthesized by successive ionic layer deposition (SILD) method are discussed. The main attention is focused on SnO_2–based metal oxides, which are promising materials for gas sensor applications. FTIR spectroscopy has shown that the precipitates of metal oxides, deposited by SILD method, are hydroxide, peroxide or hydrated metal oxide-based compounds. After annealing at relatively low temperatures (200–400°C) these compounds release both water and peroxide oxygen and transform into corresponding oxides. According to XRD, SEM and AFM measurements it was confirmed that deposited films had fine-dispersed structures. Only after annealing at T_{an}>500°C, XRD diffraction peaks, typical for nanocrystalline material with grain size < 6–8 nm, were observed. High roughness and high degree of agglomeration are important peculiarities of metal oxides deposited by SILD. Metal oxide films consist of spherical agglomerates. Degree of agglomeration of the films and agglomerate size could be controlled. It was found that introduction of various additives in the solution for SILD could sufficiently change the microstructure of synthesized metal oxides.

Keywords: *metal oxide, nanolayers, microstructure, composition, characterization*

I. Introduction

Metal oxides are materials widely used in various areas, from electronics and fuel cells to transport, medicine and construction [1–5]. Due to peculiarities of operation, each application demands specific combination of metal oxide properties, such as electro-physical, structural, optical, catalytic, etc. Moreover, every year those requirements become more multi- various. All mentioned above requires permanent search for new compositions of metal oxide materials as well as new technologies, allowing realisation of the necessary combination of desired parameters. At present, many methods of metal oxide formation are already tested, including such methods as sol-gel technology, pulsed laser deposition, spray reaction, chemical deposition, sputtering, etc. [6–11].

In present paper we discuss opportunities of Successive Ionic Layer Deposition (SILD) technology for deposition of nanostructured metal oxides. The main purpose of this work is to analyze structural and phase transformations, which are taking place in those films during synthesis and after annealing. The SILD method is based on interactive successive treatments of the

* Corresponding author (G. Korotcenkov): tel: +82 062 9702354 fax: +82 062 9702304, e-mail: *ghkoro@yahoo.com*

* Corresponding author (B. Cho): tel: +82 062 9702318 fax: +82 82 062 9702304, e-mail: *chobk@gist.ac.kr*

* Corresponding author (V.P. Tolstoy): tel: +7 812 4284104 fax: +7 812 4285712, e-mail: *vptol@yandex.ru*

substrate surface with aqueous solutions of various salts, such as acetates, chlorides and nitrates of different metals. This method permits synthesizing nano-layers of solids with predetermined thickness and controlled composition. It is also attractive for controlled functionalizing of metal oxide surface and presents good opportunities for combinatorial synthesis of metal oxides for different applications. Detailed description of this method one can find in literature [12–16].

II. Experimental details

The analysis of transformation of both structure and phase in metal oxide films synthesized by SILD method was conducted for SnO_2, CuO_2, MnO_2, ZrO_2, etc. These layers were synthesized using technological parameters described in literature [17–38]. For their deposition we used precursors indicated in Table 1. The film thickness was controlled through the number of the used deposition cycles. The average thickness of the layer synthesized after one deposition cycle is also indicated in Table 1.

The synthesized layers were studied by FTIR (Fourier transformed infrared), UV-Vis (Ultraviolet-visible), and XPS (X-ray photoelectron) spectroscopy, as well as scanning electron microscopy (SEM). In particular, the morphology and crystallographic structure of SnO_2-Au films were controlled using a Philips XL30 FEG scanning electron microscope. XP spectra were collected on the ultrahigh vacuum system equipped with hemispherical electrostatic analyzer Omicron EA125 with MgKa line ($h\nu$=1253.6 eV) for excitation. The O, Sn, Au and C lines were recorded in detail with the pass energy of 20 eV. For some XPS experiments it was also applied Perkin-Elmer 5400 PHI spectrometer operated with unmonochromatized MgKa irradiation, at a standard resolution of 0.8 eV. For FTIR study we used a FTIR spectrometer Perkin-Elmer 1760X equipped with a DTGS detector. The spectra are aver-

Table 1. Metal oxides synthesized by SILD

Metal oxides	Precursors	Chemical composition of as- deposited films	Temperature of transformation in oxide phase [°C]	Thickness after one deposition cycle [nm]	Ref.
CeO_2	$Ce(NO_3)_3 + H_2O_2$	$Ce(OH)_{4-x}(OOH)_x$	200–300	0.3–1.0	[17]
CuO_{1+x}	$Cu(NH_3)_4(NO_3)_2$ or $CuSO_4 + H_2O_2$	$Cu(OH)_{2-x}(OOH)_x$	150–200	0.3–1.5	[18,19]
MnO_2	$MnSO_4 + KMnO_4$	$MnO_2 \cdot nH_2O$		~1.0	[19,20]
ZrO_2	$Zr(SO_4)_2 + NaOH$	$Zr(OH)_4$	100–700		[21]
Fe_2O_3	$Fe(NH_3)_2(SO_4)_2 + H_2O$	FeOOH	250–300	0.3–0.5	[19,22]
ZnO	$Zn(NO_3)_2 + H_2O_2$	$Zn(OH)_{2-x}(OOH)_x$	180–220	~ 0.8	[23,24]
PbO_2	$Pb(NO_3)_2$	$PbO_2 \cdot nH_2O$			[25]
La_xNbO_y	$La(NO_3)_3 + Nb(OH)_{4-x}(OOH)_x$	$La_xNb(OH)_y$	350–400	~ 0.6	[13]
Ce_xNbO_y	$CeCl_3 + K_3NbO_8$	$Ce_xNb(OH)_y$	200–500		[26]
Co_xMnO_y		$Co_3MnO_x \cdot nH_2O$		~0.5	[27]
Ce_xMnO_y	$CeCl_3 + KMnO_4$	$Ce_4MnO_x \cdot nH_2O$			[28]
Fe_xNiO_y	$(NH_4)_2Fe(SO_4)_2 \cdot 6H_2O + NiSO_4$				[29,30]
Fe_xCrO_y		$Fe(OH)_3 + Cr(OH)_3$		~0.35	[29]
$BiVO_4$	$BiOClO_4 + NaVO_3$		300–350		[31]
SnO_2	$SnF_2 + H_2O_2$	$Sn(OH)_4$ or $SnO_2 \cdot nH_2O$	300–350	0.5–1.5	[18,32,33]
Sn_xMoO_y	$SnCl_2 + Na_2MoO_4$	$Sn_xMoO_y \cdot nH_2O$	200–400	~ 0.6	[34]
$Sn_xPW_yO_z$	$SnCl_2 + H_3PW_{12}O_{42}$	$Sn_x(OH)_yPW_zO_k$	200–500		[35]
SnO_2-Au	$SnCl_2 + HAuCl_4$				[36,37]
SnO_2-Pd	$SnCl_2 + PdCl_2$				[15]
MnO_2-Ag	$Mn(Oac)_2 \cdot 4H_2O + AgNO_3$	Ag_x-$MnO_2 \cdot nH_2O$			[38]

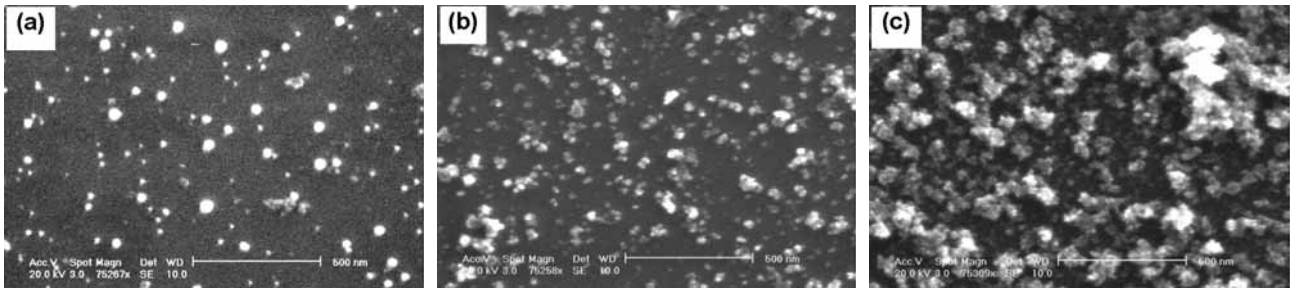

a) b) c)

Figure 1. Typical SEM images of SnO_2-Au nanocomposite films synthesized by SILD method using different number of deposition cycles: (a) 1 deposition cycle, (b) 7 deposition cycles, (c) 13 deposition cycles

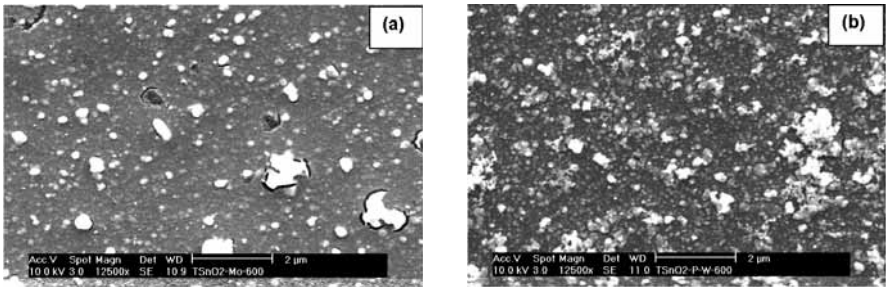

a) b)

Figure 2. SEM images of (a) $SnMo_{0.6}O_x \cdot H_2O$ and (b) $Sn_xPW_yO_z \cdot nH_2O$ films synthesized by SILD [15]
(Copyright @ Institute of Physics Publishing, 2006)

ages of 20–50 scans at a resolution of 4 cm^{-1}. UV-Vis spectra were measured with a Lambda-9 spectrophotometer (Perkin-Elmer) at a scanning rate of 50 nm/min and a slit program of 2 nm.

III. Results and discussion

3.1 Peculiarities of films growth. Film morphology

Typical SEM images of the surface morphology of metal oxide films deposited on Si substrate by the SILD method are shown in Fig. 1.

It is seen that the growth of metal oxide layers takes place through the formation of 2D and 3D precipitates uniformly distributed along the surface. Surface concentration of the precipitated species gradually increases with enlarging of deposition cycles. Research made for various metal oxides has shown that continuous coating usually has been formed only after 10–13 deposition cycles. From the SEM images of various films, synthesized by SILD method (Fig. 2), one can see that the formation of continuous nano-layers takes place uniformly over the whole surface. However, the morphology of those continuous layers is determined by the nature of synthesized material.

The analysis of SEM images has also shown that the size of precipitates, grown on the surface of the processed substrates, has wide dispersion and can vary from 5 to 40 nm. At the same time, the average size of those precipitates weakly depends on the number of deposition cycles and is about 10–15 nm. It is also established that the layers deposited by SILD method are characterized with strong agglomeration of the

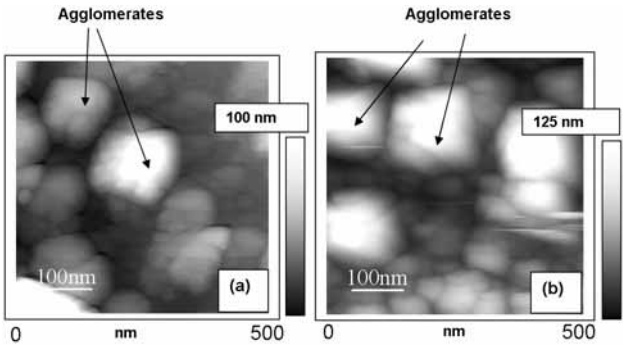

a) b)

Figure 3. AFM images of (a) SnO_2 and (b) SnWPO films deposited by SILD (T_{an} = 600°C) [15]
(Copyright @ Institute of Physics Publishing 2006)

precipitates indicated above. According to SEM and AFM measurements, these agglomerates have spherical shape (see Fig. 3).

Due to high agglomeration films deposited by SILD have higher roughness in comparison to the roughness of tin oxide films deposited by standard methods of film deposition [39–41]. For example, the SnO_2 films deposited by SILD method had 2–3 times higher roughness than the SnO_2 films deposited by spray pyrolysis method [39], and 3–4 times higher than the SnO_2 films deposited by low temperature sputtering technology and electron beam evaporation [40,41].

SEM images clearly indicate also that the size of agglomerates goes up when the increasing of the metal oxide film thickness takes place. For example, for the SnO_2 films deposited by SILD method, agglomerate

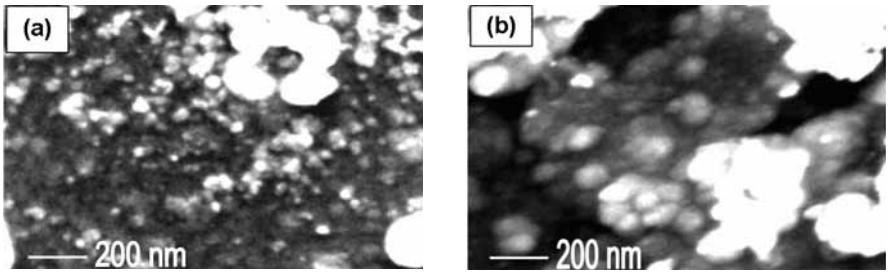

a) b)

Figure 4. SEM images of SnO_2 films deposited on sintered quartz substrate in dependence on the number of deposition cycles: a) 20, b) 40 deposition cycles [33]
(Copyright @ Elsevier, 2003)

sizes are increased from 20 to 300 nm when the number of deposition cycles is enlarged from 10 to 40 (see Figs. 4 and 5). For the SnO_2-Au nanocomposites the average size of agglomerates reaches ~100 nm after 16 deposition cycles [36,37]. It indicates that the growth of the metal oxide films during deposition from aqueous solutions takes place through the growth of the agglomerates.

After annealing of the synthesized films we have observed some increase of the average size of agglomerates. For example, in the SnO_2 films synthesized using 30 deposition cycles, after annealing at T_{an}=600°C the average size of agglomerates has been increased from 60 nm to 80 nm [33]. However, even after annealing at T_{an}=800°C, films conserved their rough "macrostructure" without noticeable changes. It is necessary to note that this conclusion is not related to the "microstructure" of the studied SnO_2 films, i.e. to the structure and size of individual crystallites, which form these agglomerates.

One should note that such structural peculiarities as high level of agglomeration and small grain size, exposed for the SnO_2 films, have found a confirmation in the results of research of other metal-oxide films, synthesized by SILD method. In particular, the same results we have obtained during research of structural properties of such nano-composite films as SnO_2-MoO_3 and $Sn_xW_yPO_z$ (see Fig. 6) [15,35]. It means that established dependences are common regularities for SILD coverings.

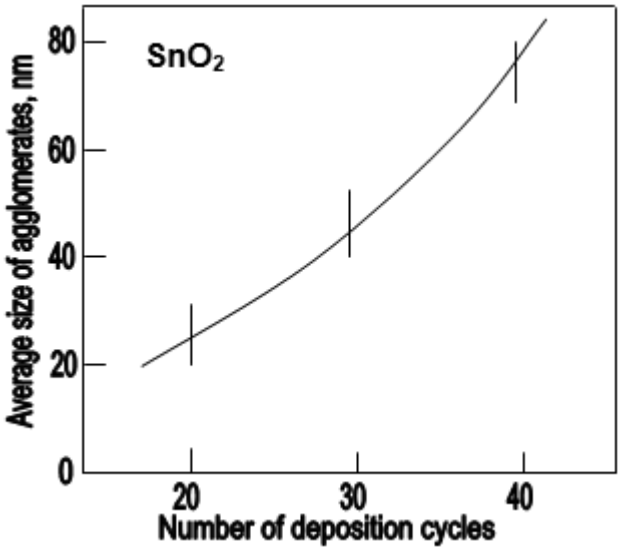

Figure 5. The influence of the number of deposition cycles on the average size of agglomerates in SnO_2 films deposited by SILD [33]
(Copyright @ Elsevier, 2003)

It is necessary to note that either the level of agglomeration of the films, obtained by SILD method, or agglomerate size could be controlled. We have found out that introduction of various additives in the solution for SILD could sufficiently change the microstructure of metal oxide matrix. As an example of such influence one can consider SEM images of SnO_2, SnO_2 : MoO_3, SnO_2 : Au and SnO_2 : Pd films

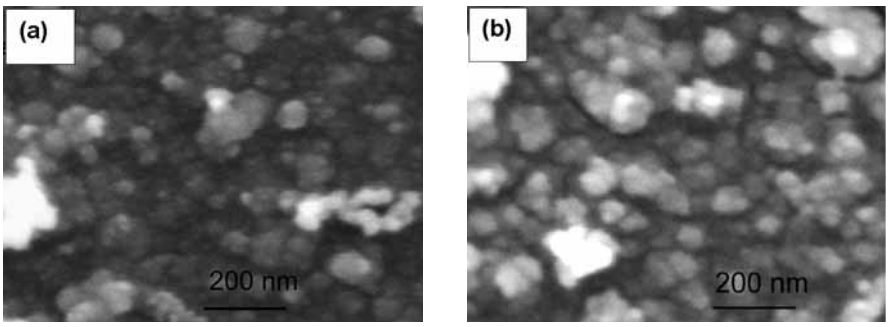

a) b)

Figure 6. SEM images of a Sn–P–W–O nanolayer deposited on silicon before (a) and after (b) heating at 600°C (30 deposition cycles). The images were obtained for different areas of the sample [35]
(Copyright @ Elsevier, 2003)

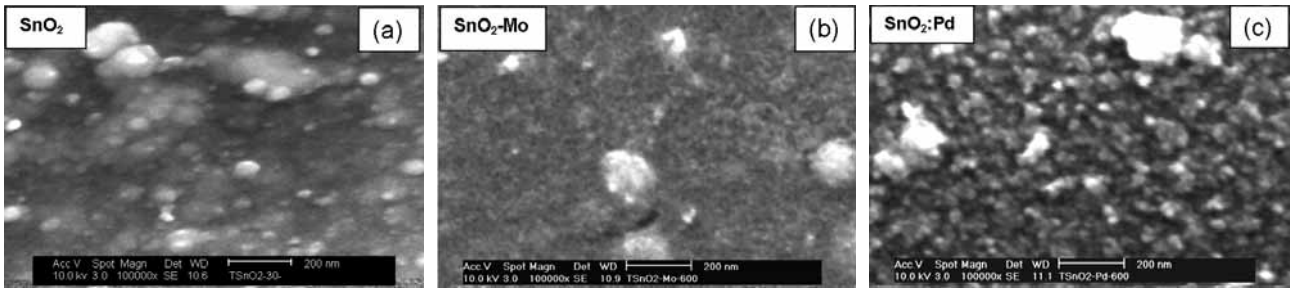

a) b) c)

Figure 7. SEM images of (a) SnO_2, (b) SnO_2:MoO_2, and (c) SnO_2:Pd films synthesized by SILD method at the surface of oxidized Si (111) substrate [15]
(Copyright @ Institute of Physics Publishing, 2006)

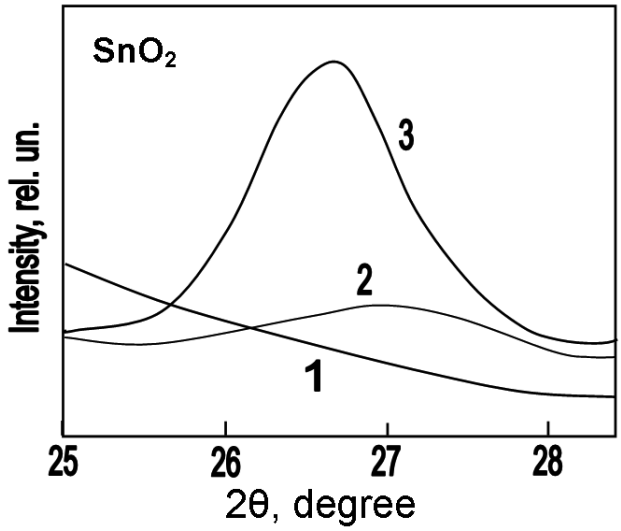

Figure 8. The influence of thermal annealing on the shape of smoothed XRD patterns of SnO_2 films synthesized by SILD. XRD patterns were measured in the region of main peak, corresponded to X-ray diffraction on the SnO_2(110) plane: (1) as-deposited, (2) T_{an}=600°C, (3) T_{an}=800°C [15]
(Copyright @ Institute of Physics Publishing, 2006)

synthesized by SILD method shown in Figs. 1 and 7. Precursors used for the deposition of those films are given in Table 1. However, this research is at its initial stage, therefore it is too early to say anything about established regularities.

3.2 Structural characterization of metal oxide films deposited by SILD

According to XRD measurements, metal oxide films deposited by SILD method are fine-dispersed formations. Usually on XRD patterns of as-deposited films we do not observe any diffraction peaks [33]. Only after annealing at T_{an} > 300–500°C in XRD patterns we are starting to observe XRD diffraction peaks, typical for polycrystalline material [32,33].

Analysis of the shape of XRD patterns has shown that the position of XRD diffraction peaks on XRD patterns and the ratio of these peaks intensities correspond to metal oxides without any preferred orientation. It indicates that the substrate does not have exerted orientation influence on the growth of crystallites during SILD. However, we can not contend that the substrate does not influence on the crystallite growth at all. For example, comparing the SEM images of the SnO_2 films deposited on Si and quartz substrates, we have found out that films deposited on Si substrate consist of larger agglomerates.

When T_{an} increases, the peaks observed in XRD patterns become more narrow and intense [31,33]. For the SnO_2 films this effect is clearly observed for the most intensive XRD peak, corresponding to diffraction at the SnO_2(110) surface (see Fig. 8). This observed evolution indicates on crystallite growth during the heat treatment.

However, even after annealing at T_{an}=800°C, the size of crystallites calculated using Scherrer's formula does not exceed 6–7 nm, which is much less than the average size of agglomerates (~75 nm). Thus, even at T=800°C, we do not observe the coalescence of crystallites, forming agglomerates. Such peculiarity is an important advantage of the SnO_2 films formed by SILD technology. For comparison, the SnO_2 films prepared by RGTO (Reothaxial Growth and Thermal Oxidation) technology have the same "macrostructure" of the films. However, already at T_{ox}=450°C the size of crystallites forming these films exceeds 10 nm [42].

In the SnO_2 powders prepared by sol-gel technology under the same conditions of annealing, the grain size increases from 3–5 nm to 13–18 nm [43].

The same transformations were observed for other metal oxides synthesized by SILD method. For ex-

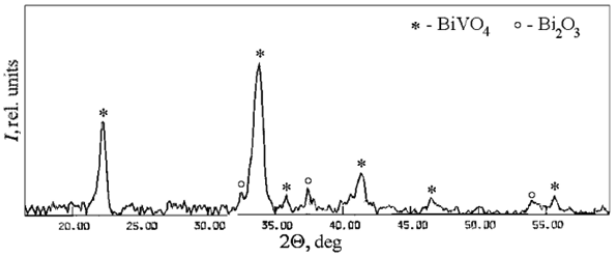

Figure 9. XRD pattern of $BiVO_4$ nanolayer on silicon surface. $C_{BiOClO4}$= 0.01 M, C_{NaVO3}= 0.01 M, $pH_{BiOClO4}$=pH_{NaVO3}=3, τ_{treat}= 30 s, τ_{wash}= 30 s, N_{SILD} = 40, $T_{heating}$= 350°C [31]
(Copyright @ Elsevier, 2002)

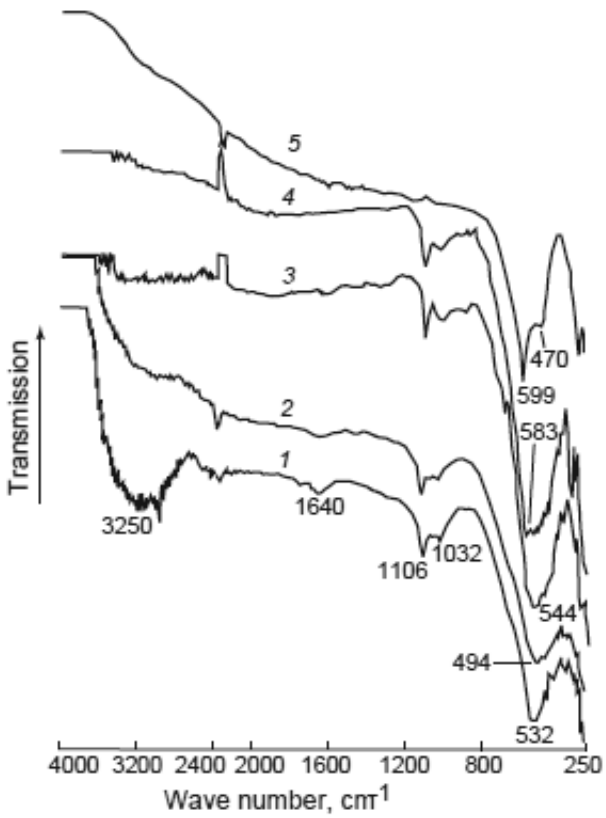

Figure 10. The influence of thermal treatments on the FTIR transmission spectra of SnO_2 films deposited on Si substrates (40 deposition cycles; t_{an}=15 min): (1) as-deposited films, (2) T_{an}=200°C, (3) T_{an}=400°C, (4) T_{an}=500°C, (5) SnO_2 films deposited by spray pyrolysis (T_{pyr}= 450°C; *d*~ 200 nm) [33]
(Copyright @ Elsevier, 2003)

ample, XRD patterns shown in Fig. 9 indicate that the Bi–V–O-containing nanolayers, after annealing at T_{an}=350°C, transform in polycrystalline $BiVO_4$ with additives of Bi_2O_3 [31].

3.3. Phase composition of the films deposited by SILD and phase transformations in the metal oxide phase during thermal treatments

IR spectroscopy of metal oxides deposited by SILD method testifies that as-deposited films present a formation of hydroxide or hydrated metal oxide-based compounds [34,35]. For example, in case of the SnO_2 deposition the formation of such compounds as tin hydroxide or hydrated tin dioxide ($Sn(OH)_4$ or $SnO_2 \cdot nH_2O$) takes place on the surface of the substrate. The broad band on FTIR transmission spectra (Fig. 10) centred around 3250 cm^{-1} is a confirmation of this conclusion. According to literature data [13], the fundamental vibration ν_{OH}(Sn-OH) lays in this frequency region (2900–3700 cm^{-1}).

The same situation one can observe with other metal oxides (see Table 1). For example, the results of differential diffuse reflectance FTIR spectra (DRIFTS) study of iron-containing coating synthesized on the silica gel surface are shown in Fig. 11. As it is seen from these spectra, the films after 8 SILD cycles are characterized with a wide band at about 1000 cm^{-1}, assignable to the bending vibration of Fe–OH groups, as well as a wide band in the 800–400 cm^{-1} region. The appearance of the last band is initiated by the stretching vibrations of the Fe–O bonds, which are broadened and overlapped due to a low crystallinity state of the layer [44]. It is necessary to note that indicated spectrum is similar to published spectra of low crystalline ferric hydroxides [45].

The results of FTIR study of cuprous oxide phase synthesized by SILD are shown in Fig. 12. A FTIR spectra of these layers synthesized on a silicon surface show that they are cuprous hydroxy-peroxide nanolayers. The presence of bands at 3390 cm^{-1} and 1640 cm^{-1}, appearing due to the stretching and bending modes of OH-groups of adsorbed water, indicates on this fact. In addition, a series of bands are being observed in the 1550–1400 cm^{-1} region. These bands can be ascribed to either the bending modes of hydroxyl groups in CuOH and CuOOH structural units or, which is more realistic, to the stretching vibrations of the C–O groups of carbonate. Finally, a band at 850 cm^{-1} can be attributed to the stretching vibrations of the –O–O– bonds.

The results of FTIR and XPS study of deposited films, presented in recent papers [31,33,35] have shown that during annealing at relatively low temperatures (200–400°C), these compounds release both water and peroxide oxygen and transform into corresponding oxides. The main part of the coordinated water, which can be responsible for the appearance of corresponding bands in FTIR spectra, is being removed from the film already after annealing at T_{an} = 200°C. For example, as it is seen for the SnO_2 films (see Fig. 10, curve 2), after annealing of synthesized films in the air at 200°C the intensity of the water bands abruptly decreases, whereas the peroxide band at 846 cm^{-1} vanishes. At the same time, the δ(OH) bands in the 1500–1300 cm^{-1} region are still observed, disappearing only after sample annealing at 500°C (Fig. 10, curve 4). The disappearance of the peroxide band undoubtedly indicates that the peroxide compound, synthesized during SILD process, decomposes. However, it is necessary to note that the traces of the water hydroxyl groups remain even after annealing at T_{an} = 500°C.

There are also noticeable changes of FTIR spectra in the region of valence Sn-O bonds (300–700 cm^{-1} [33]) taking place already at T_{an} > 200°C. Exactly at T_{an} = 200°C, we observe a shift of this absorbance peak from 532 cm^{-1} to 494 cm^{-1} with further shifting to 544 cm^{-1} at T_{an} = 400°C, and to 583 cm^{-1} at T_{an} = 500°C. Such transformation of FTIR spectra indicates that already at T_{an} = 200°C both micro-structural changes, and the changes of space symmetry take place in the deposited films. Observed changes are the result of the hydroxide conversion to tin dioxide. Possibly, these phase transformation are responsible for some increase of the agglomerate size, which is observed af-

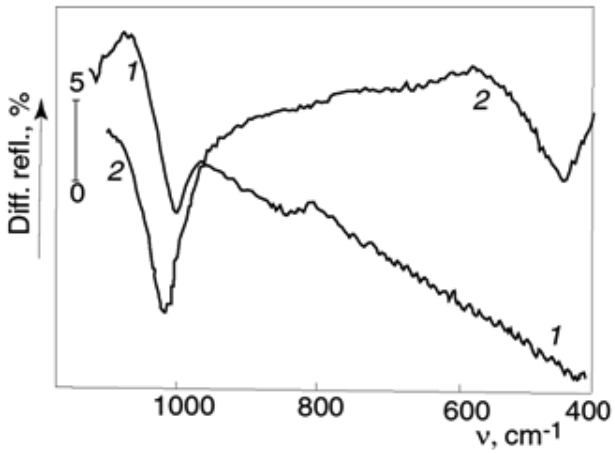

Figure 11. DRIFTS of the ferric (hydr)oxide layer deposited on silica gel by eight SILD cycles: (1) air dried sample, (2) sample after subsequent heating at 250°C for 0.5 h. The spectra were obtained by subtracting the DRIFTS spectrum of the initial silica gel from those of the treated samples

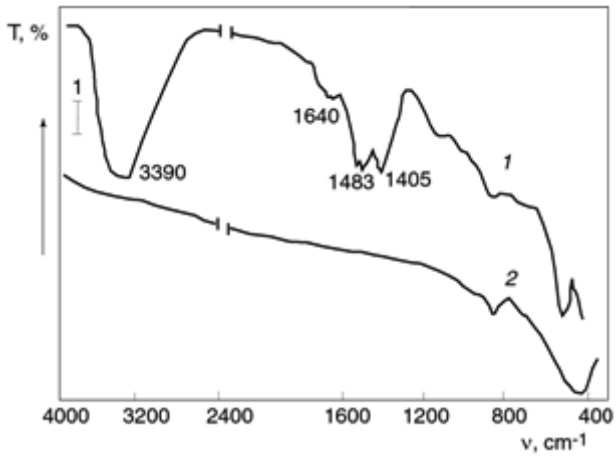

Figure 12. FTIR transmission spectra of the $CuO_{1+x}\cdot nH_2O$ nanolayers deposited on a silicon plate by forty SILD cycles: (1) as-synthesized sample, (2) sample after subsequent heating in air at 300°C

ter annealing at T_{an} =600°C. However, in contrast to FTIR transmission spectra of the SnO_2 films deposited by spray pyrolysis (Fig.10, curve 5), in FTIR spectra of the SnO_2 films deposited by SILD we have not observed the splitting of indicated absorbance peak in the region 500–700 cm^{-1} into two bands even after annealing at T_{an} = 500°C (Fig. 10, curve 4). FTIR transmission spectra of the SnO_2 films deposited by the low temperature spray pyrolysis have a narrow peak at 599 cm^{-1} and a shoulder at 470 cm^{-1} in this spectral region. Such behaviour of the Sn-O absorbance peak, and considerable broadening of this band in comparison with the Sn-O absorbance peak of the SnO_2 polycrystalline films (t = 20–40 nm) confirms our conclusion that the structure of the SnO_2 films prepared by SILD technology is fine-dispersed even after annealing at T_{an}=500°C. The possibility to form such nanosize films is a great advantage of this SILD method.

For Fe_2O_3 oxides, a consequence of transition in the oxide phase is the appearance of the band at 450 cm^{-1} (see Fig. 11), assignable to the stretching Fe–O vibrations of ferric oxide octahedrons [44].

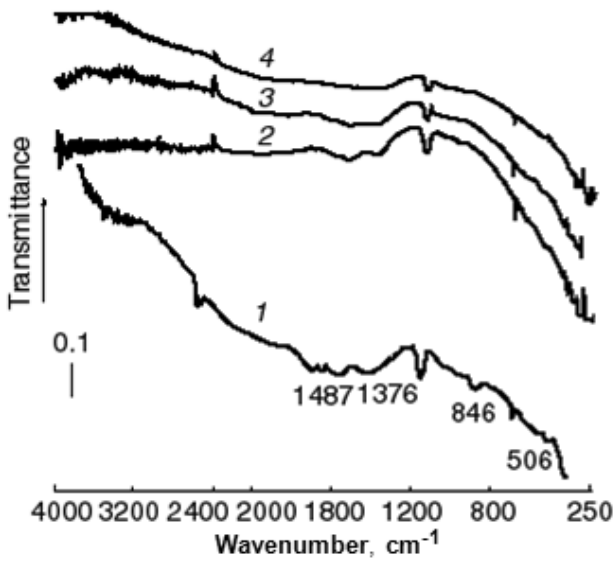

Figure 13. FTIR transmission spectra of $Ce_{0.74}NbO_x\cdot nH_2O$ nanolayers (1) as-deposited at the surface of single crystalline silicon by 25 SILD cycles and after annealing at (2) 200°C, (3) 300°C, (4) 500°C during 0.5 h [15]
(Copyright @ Institute of Physics Publishing, 2006)

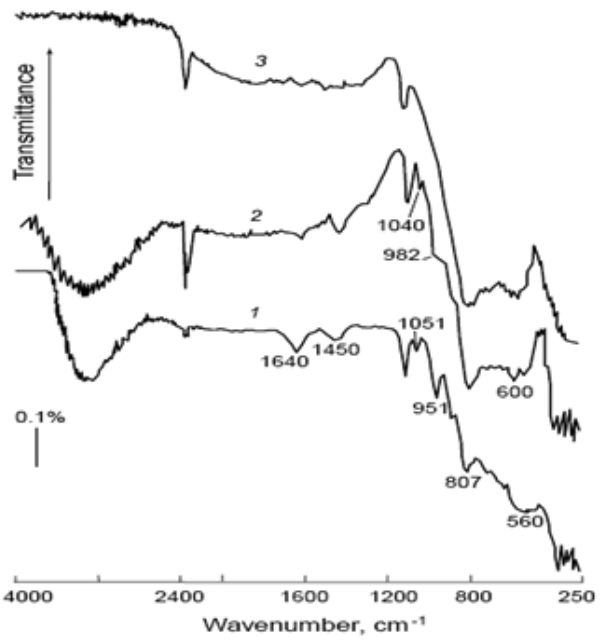

Figure 14. FTIR transmission spectra of a Sn–P–W–O nanolayer as-deposited on a surface of crystalline silicon by: (1) 30 SILD cycles, (2) heated at 200°C for 0.5 h, (3) heated at 500°C for 0.5 h [35]
(Copyright @ Elsevier, 2003)

For the $Ce_{0.74}NbO_x \cdot nH_2O$ films, synthesized at the Si surface, the results of this process are shown in the Fig. 13. We see that after annealing the intensity of absorption bands, connected with the presence of the different hydroxide or hydrated metal oxide-based compounds in analyzed films sharply drops [46]. As it is known, a broad absorption band at 3500–3200 cm^{-1} is conditioned by the stretching (ν) modes of OH groups in both hydroxide and physisorbed water, a band at 1640 cm^{-1} is typical for the bending (δ) mode of water, bands at 1487 cm^{-1} and 1376 cm^{-1} are conditioned by the δ(OH) modes of niobium and cerium hydroxides, and a band at 846 cm^{-1} is assigned to the O–O stretches in the adsorbed peroxide species.

Analogous processes also take place in other metal oxide phases, synthesized by SILD [14]. As it is seen in the Fig. 14, after heating of the sample in the air at 200°C (Fig. 14, curve 2), the absorption bands of molecular water decrease in the intensity, the nPO_4 band at 1051 cm^{-1} shifts to 1040 cm^{-1}, the 951 cm^{-1} band shifts to 982 cm^{-1} and decreases, the absorption band in the 780–800 cm^{-1} range increases and broadens, while the 560 cm^{-1} band significantly decreases. The δ_{M-OH} band and the water bands disappear at 300°C and 400°C respectively (spectra are not shown). The following heating at 400–500°C (Fig. 14, curve 3) results in the disappearance of the 982 cm^{-1} band, while the bands at 550–600 $cm^{-1}$and 780–800 cm^{-1}, which can be conditioned by the W–O and W–O–Sn modes, become dominant in the spectra. Those spectral changes are consistent, on the one hand, with condensation of the Sn–OH and W–OH bonds and on the other hand with rapture of the $W_{1/4}O$ and Sn–O–Sn bonds and formation of such new chemical bonds as W–O–W, or W–O–Sn.

Thus, presented results testify that peculiarities of phase transformation, established for the SnO_2 films, are general for all metal oxides, synthesized by SILD method.

IV. Conclusions

The analysis of morphology of metal oxides synthesized by successive ionic layer deposition (SILD) method has shown that high degree of agglomeration is an important peculiarity of metal oxides, deposited by SILD. Metal oxide films deposited by the SILD method have high roughness and they consist of spherical agglomerates. The degree of agglomeration of the films and agglomerates' size could be controlled. It was found that introduction of various additives in the solution for SILD could sufficiently change the microstructure of synthesized metal oxides.

According to XRD, SEM and AFM measurements deposited films are fine-dispersed formations. Only after annealing at T_{an} > 300–500°C in XRD patterns we start observing XRD diffraction peaks, typical for nanocrystalline material with grain size < 6–8 nm.

FTIR spectroscopy has shown that metal oxides deposited by SILD method are various forms of hydroxide, peroxide or hydrated metal oxide-based compounds. After annealing at relatively low temperatures (200–400°C), these compounds release both water and peroxide oxygen, and transform into corresponding oxides.

Acknowledgements: G. Korotcenkov is thankful to Korean BK21 Program; and V. Tolstoy is thankful to Russian Foundation for Basic Research for support of research. G. Korotcenkov is also thankful to COST for supporting his participation in COST Meeting. The authors are also thankful to Dr. L. Gulina and Dr. E. Tolstobrov from University of St.-Petersburg for synthesizing of some samples; to Prof. J. Schwank from University of Michigan and Dr. V. Brinzari from Technical University of Moldova for their help in structural and surface characterization of studied films.

References

1. C.G. Granqvist, "Electrochromic devices", *J. Eur. Ceram. Soc.*, **25** (2005) 2907–2912.
2. C. Grivas, R. Weason, "Dielectric binary oxide films as waveguide laser media: a review", *J. Phys.: Condens. Matter*, **20** (2008) 264011.
3. S.M. Haile, "Fuel cell materials and components", *Acta Mater.*, **51** (2003) 5981–6000.
4. G. Korotcenkov, "Metal oxides for solid state gas sensors. What determines our choice?", *Mater. Sci. Eng.* B, **139** (2007) 1–23.
5. I.E. Wachs, "Recent conceptual advances in the catalysis science of mixed metal oxide catalytic materials", *Catal. Today*, **100** (2005) 79–94.
6. P.R. Willmott, "Deposition of complex multielemental thin films", *Prog. Surf. Sci.*, **76** (2004) 163–217.
7. S.H. Park, Y.C. Son, W.S. Willis, S.L. Suib, K.E. Creasy, "Tin oxide films made by physical vapor deposition - Thermal oxidation and spray pyrolysis", *Chem. Mater.*, **10** (1998) 2389–2398.
8. L. Besra, M. Liu, "A review on fundamentals and applications of electrophoretic deposition (EPD)", *Prog. Mater. Sci.*, **52** (2007) 1–61.
9. T.P. Niesen, M.R. De Guire, "Review: Deposition of ceramic thin films at low temperatures from aqueous solutions", *J. Electroceram.*, **6** (2001) 169–207.
10. A.C. Pierre, *Introduction to Sol Gel Processing.* Kluwer Academic Publ., Boston, 1998.
11. A.C. Jones, P. O'Brien, *CVD of Compound Semiconductors. Precursor Synthesis, Development and Applications.* Wiley/VCH, Weinheim, 1997.
12. V.P. Tolstoy, "Successive ionic layer deposition. The use in nanotechnology", *Rus. Chem. Rev.*, **75** (2006) 161–175.
13. V. Tolstoy, "The peroxide route of the successive ionic layer deposition procedure for synthesis nanolayers of metal oxides, hydroxides and peroxides", *Thin Solid Films*, **307** (1997) 10–13.

14. V. Tolstoy, S.D. Han, G. Korotcenkov, "Successive ionic layer deposition (SILD): advanced method for deposition and modification of functional nanostructured metal oxides aimed for gas sensor applications", Chapter in *Metal Oxide Nanostructures and Their Applications*. Eds. A. Umar, Y.B. Hahn**,** American Scientific Publishers, California, USA, (2008) (in press).
15. G. Korotcenkov, V. Tolstoy, J. Schwank, "Successive ionic layer deposition (SILD) as a new sensor technology: Synthesis and modification of metal oxides", *Meas. Sci. Techn.*, **17** (2006) 1861–1869.
16. G. Korotcenkov, V. Tolstoy, J. Schwank, I. Boris, "Successive ionic layer deposition: Possibilities for gas sensor applications", *J. Phys.: Confer. Series (IOP)*, **15** (2005) 45–50.
17. V. Tolstoy A. Enrlich, "The synthesis of $CeO_{2+n}\cdot nH_2O$ nanolayers on silicon and fused-quartz surfaces by the successive ionic layer deposition technique", *Thin Solid Films*, **307** (1997) 60–65.
18. V. Tolstoy, E. Molotilkina, "The Synthesis on silica surface by SILD of $SnO_2\cdot nH_2O$ nanolayers", *Russ. J. Inorg. Chem*., **38** [3] (1993) 388–391.
19. G. Korotcenkov, V. Macsanov, V. Brinzari, V. Tolstoy, J. Schwank, A. Cornet, J. Morante, "Influence of Cu, Fe, Co, and Mn oxide nanoclusters on sensing behavior of SnO_2 films", *Thin Solid Films*, **467** [1-2] (2004) 209–214.
20. V. Tolstoy, I. Murin, A. Reller, "Synthesis of Mn(IV) oxide nanolayers by successive ionic layer deposition, *Appl. Surf. Sci*., **112** [2] (1997) 255–257.
21. S. Park, B. Clark, D. Keszler, J. Bender, J. Wager, Th. Reynolds, G. Herman, "Low-temperature thin-film deposition and crystallization", *Science*, **297** (2002) 65.
22. V. Tolstoy, "The LbL synthesis on silica surface of FeOOH nanolayers", *Rus. J. Appl. Chem*., **72** [8] (1999) 1259–1262.
23. E. Tolstobrov, V. Tolstoy, "The synthesis on silica surface by SILD of $ZnO_{1+x}\cdot nH_2O$ nanolayers", *Rus. J. Appl. Chem*., **68** [6] (1995) 1018–1020.
24. S. Lindroos, M. Leskela, "Growth of zinc peroxide (ZnO_2) and zinc oxide (ZnO) thin films by the SILAR-technique, *Int. J. Inorg. Mater*., **2** [2-3] (2000) 197–201.
25. V.P. Tolstoi, E.V. Tolstobrov, "Synthesis of highly oriented α-PbO_2 layers on the surfaces of single-crystal silicon and quartz by successive ionic layer deposition", *Rus. J. Appl. Chem.*, **75** [9] (2002) 1529–1531.
26. V. Tolstoy, L. Gulina, E. Tolstobrov, "Synthesis of metal-oxide, metal-hydroxide, and metal-peroxide nanolayers by successive ionic layer deposition method from solution", *Proceedings of Electrochem. Soc.*, **32** (2003) 209–214.
27. L.B. Gulina, V.P. Tolstoy, I.V. Murin, "Study of COMnO- and LiCoMnO-containing layers synthesized by successive ionic layer deposition on silica surface", *Rus. J. Appl. Chem*., **74** [11] (2001) 1955–1957.
28. V.P. Tolstoi, "Synthesis of $Ce_4MnO_x\cdot nH_2O$ layers on silica gel surface by ionic layer deposition", *Rus. J. Appl. Chem.*, **75** [4] (2002) 656–658.
29. V.P. Tolstoi, I.V. Stepanenko, "Redox reactions in the layer of adsorbed Fe^{2+} and CrO_4^{2-} ions and synthesis of Fe^{3+}-Cr^{3+} double hydroxide nanolayers by ionic deposition", *Rus. J. Gen. Chem*., **75** [1] (2005) 46–48.
30. V.P. Tolstoi, I.V. Damsonova, "Synthesis of nanolayers of double Fe(III) and Ni(II) hydroxide by ionic layer deposition on quartz and silicon surfaces", *Rus. J. Appl. Chem*., **76** [9] (2003) 1396–1398.
31. V.P. Tolstoy, E.V. Tolstobrov, "The synthesis of Bi–V–O-containing nanolayers on silica surfaces by the successive ionic layer deposition technique", *Solid State Ionics*, **151** (2002) 165–169.
32. V. Tolstoy, "The Synthesis by SILD of $SnO_2\cdot nH_2O$ nanolayers", *Rus. J. Inorg. Chem*., **38** [7] (1993) 1146–1148.
33. G. Korotcenkov, V. Macsanov, V. Tolstoy, V. Brinzari, J. Schwank, G. Faglia, "Structural and gas response characterization of nano-size SnO_2 films deposited by SILD method", *Sens. Actuators*, **B 96** [3] (2003) 602–609.
34. L. Gulina, V. Tolstoy, "Synthesis by SILD of $Sn_{0.6}MoO_y\cdot nH_2O$ nanolayers on silica", *Thin Solid Films*, **440** (2003) 74–77.
35. V. Tolstoy, L. Gulina, G. Korotcenkov, V. Brinzari, "Synthesis of nanolayers of hybrid-type hydroxo-SnOH and heteropoly-$H_xPW_yO_z$ compounds on silica surfaces by successive ionic layer deposition method", *Appl. Surf. Sci*., **221** [1-4] (2003) 197–202.
36. G. Korotcenkov, V. Tolstoy, L. Gulina, I. Blinov, J. Schwank, "SnO_2-Au^0 nanocomposite synthesized by SILD method: Structural and gas sensing characterization", p. 155 in *Proceedings of 1st Int. Symp. Transparent Conducting Oxides - TCO*-2006, Crete, Greece 2006.
37. V. Tolstoy, L. Gulina, G. Korotcenkov, "Nanolayers of the Au^0-SnO_2 nanocomposite synthesized by successive ionic layer deposition method", pp. 239–241 in *Proceeding of the 4th Int. Conf. Microelectronics and Computer Science*, Chisinau, Moldova, Vol. 1, 2005.
38. V. Tolstoy, E. Tolstobrov, "The Synthesis by SILD of Ag^0-$MnO_2\cdot nH_2O$ nanolayers", *Russ. J. Gen. Chem*., **74** [3] (2004) 360–365.
39. V. Brinzari, G. Korotcenkov, V. Golovanov, J. Schwank, V. Lantto, S. Saukko, V. Golovanov, "Morphological rank of nano-scale tin dioxide films deposited by spray pyrolysis from $SnCl_4\cdot 5H_2O$ water solution", *Thin Solid Films*, **408** [1–2] (2002) 51–58.
40. R. Doblec, M.A. ElKhakari, A.M. Serventi, M. Trudeau, R.G. Saint-Jacques, "Microstructure and physical properties of nanostructured tin oxide thin films grown by means of pulsed laser deposition", *Thin Solid Films*, **419** (2002) 230–236.
41. X.Q. Pan, L. Fu, "Tin oxide thin films growth on the (1012) sapphire substrate", *J. Electroceram.*, **7** (2001) 35–46.
42. G. Sberveglieri, S. Groppelli, P. Nelli, C. Perego, G. Valdré, A. Camanzi, "Detection of sub-ppm H_2S concentrations by means of SnO_2(Pt) thin films, grown by the RGTO technique", *Sens. Actuators*, B **15** [1-3] (1993) 86–89.

43. C.H. Shek, J.K.L. Lai, G.M. Lin, "Grain growth in nanocrystalline SnO_2 prepared by sol-gel route", *Nanostruct. Mater.*, **11** (1999) 887–893.
44. W. Sung, J.J. Morgan, "Kinetics and products of ferrous iron oxygenation in aqueous systems", *Env. Sci. Technol.*, **14** (1980) 561–568.
45. Y. Aoi, H. Kambayashi, T. Deguchi, K. Yato, S. Deki, "Synthesis of nanostructured metal oxide by liquid-phase deposition", *Electrochim. Acta*, **53** (2007) 175–178.
46. K. Nakamoto, *Infrared and Raman Spectra of Inorganic and Coordination Compounds,* 4th ed. Wiley, Chichester, 1986.